The Quadruple Chains of SbO_6 Octahedra in $Sb_2Te_2O_9$: an Example of Low Extent of Aggregation of Pentavalent Antimony Polyhedra†

José Antonio Alonso,[a] Alicia Castro,*[a] Renée Enjalbert,[b] Jean Galy[b] and Isidoro Rasines[a]

[a] *Instituto de Ciencia de Materiales de Madrid, C.S.I.C., Serrano 113, 28006 Madrid, Spain*

[b] *Centre d'Elaboration de Matériaux et d'Etudes Structurales, C.N.R.S., 29 rue Jeanne Marvig, 31055 Toulouse Cedex, France*

Single crystals of $Sb_2Te_2O_9$ have been grown by transport methods, and the crystal structure determined by X-ray single-crystal techniques. The results have been confirmed by a neutron powder diffraction refinement. The compound crystallizes in the monoclinic system, space group $P2_1/c$, $Z = 8$, with unit-cell parameters $a = 21.79(1)$, $b = 4.849(1)$, $c = 14.574(9)$ Å and $\beta = 109.21(3)°$. The structure consists of infinite quadruple chains of vertex-sharing $Sb^{V}O_6$ octahedra, running along the b axis, bridged by $(Te_6O_{26})_\infty$ strings parallel to the [0 0 1] direction and by isolated Te_2O_{10} groups. The Te^{IV} is five- and six-co-ordinated by oxygen, in very irregular environments making room for the free electron pairs. This structure is discussed in the framework of other pentavalent antimony complex oxides and contrasted with those of the known oxides in the M_2O_5–TeO_2 (M = V, Nb or Ta) systems.

Mixed oxides containing semimetallic p elements in low oxidation state, such as Se^{IV}, Sb^{III} or Te^{IV}, exhibit crystal structures with remarkably irregular oxygen co-ordination polyhedra for these elements, due to the presence of the electronic lone pair which occupies[1] a volume approximately equivalent to that of an oxygen atom. Systematic investigations have been performed in order to study the stereochemical influence of the lone pair in new oxides containing Te^{IV}.[2–6] Usually Te^{IV} shows three- or four-co-ordination, in trigonal-pyramidal or trigonal-bipyramidal configuration, respectively, with the lone pair directed towards the unoccupied position of both polyhedra. Two or more more units are, very often, linked together to give groups of composition Te_2O_5, Te_3O_8, Te_4O_{11}, *etc.* The degree of aggregation of these units is strongly dependent on the character of the metal M atom in different M–Te–O oxides.

A beautiful example is the gradual increase in both the tellurium co-ordination and the degree of aggregation of the tellurium polyhedra in compounds of the system M_2O_5–TeO_2 (M = V, Nb or Ta) from $V_2Te_2O_9$ to $Ta_2Te_2O_9$. In $V_2Te_2O_9$[2] all the tellurium atoms are three-co-ordinated, the trigonal pyramids sharing corners to give isolated Te_2O_5 units; the three- and four-co-ordinated Te atoms in $Nb_2Te_3O_{11}$[3] form Te_3O_8 groups, whereas in $Ta_2Te_2O_9$[4] the two kinds of Te polyhedra, trigonal bipyramid and distorted octahedron, constitute two-dimensional nets of composition $(Te_4O_{12})_n$.

In order to study the influence of replacing the mentioned d metals in this family by pentavalent p elements, it seemed interesting to grow crystals of the corresponding antimony(v) compound and to study its structure. The synthesis of $Sb_2Te_2O_9$ and Sb_2TeO_7 as well as a study of the thermal behaviour and the infrared spectra have been previously described.[7] In the present work single crystals of $Sb_2Te_2O_9$ were grown by transport methods. This paper describes the crystal structure,

Table 1 Physical and crystallographic data and parameters for data collection and refinement

Formula	O_9Sb_2Te
M	642.7
Crystal system	Monoclinic
Space group	$P2_1/c$
a/Å	21.79(1)
b/Å	4.849(1)
c/Å	14.574(9)
β/°	109.21(3)
U/Å^3	1454(1)
Z	4 × 2
D_c/g cm^{-3}	5.87
F(000)	2224
μ(Mo-Kα)/cm^{-1}	157
T/K	293
λ(Mo-Kα)/Å	0.710 69
Monochromator	Graphite
Take-off angle/°	3.8
Detector width/mm	4 × 4
Scan type	ω–2θ
Scan width/°	0.70 + 0.35 tanθ
Prescan speed/° min^{-1}	10
Final scan σ(I)/I	0.018
Maximum time/s	60
Reflections for cell refinement	25; θ 6–16°
Recorded reflections	3972, θ ⩽ 30°
hkl range	0–30, 0–6, −20 to 20
Intensity-control reflections	410, 008, 235 every 3600 s
Orientation control reflections	913, 1410, 020 every 250 reflections
Independent reflections	3798
Transmission coefficient range	0.71–1.00
Empirical absorption correction	Ref. 8
Significant reflections	3713 with $I > 3\sigma(I)$
Refined parameters	146
Extinction II (g)	6.5 × 10^{-4}
R	0.041
R'	0.055
w	7.65/(σ^2F + 0.07F^2)
S	0.99

† *Supplementary data available:* see Instructions for Authors, *J. Chem. Soc., Dalton Trans.*, 1992, Issue 1, pp. xx–xxv.

Table 2 Positional parameters for the X-ray and neutron refinements

	X-Ray			Neutron		
Atom	*x*	*y*	*z*	*x*	*y*	*z*
Sb(1)	0.054 58(3)	0.718 8(1)	0.719 77(4)	0.054 7(5)	0.715(2)	0.719 6(7)
Sb(2)	0.158 06(3)	0.219 0(1)	0.666 24(4)	0.160 0(5)	0.223(2)	0.665 7(7)
Sb(3)	0.347 18(3)	0.713 8(1)	0.510 82(4)	0.346 4(6)	0.716(2)	0.509 5(8)
Sb(4)	0.447 50(3)	0.216 9(1)	0.669 20(4)	0.448 8(5)	0.217(2)	0.671 0(8)
Te(1)	0.062 44(3)	0.666 5(1)	0.947 54(4)	0.063 0(4)	0.673(2)	0.947 7(7)
Te(2)	0.233 23(3)	0.321 5(1)	0.919 47(4)	0.232 9(5)	0.319(2)	0.920 9(7)
Te(3)	0.440 45(3)	0.159 7(1)	0.890 69(4)	0.441 1(4)	0.161(2)	0.889 6(6)
Te(4)	0.279 98(3)	0.669 3(1)	0.690 32(4)	0.281 7(5)	0.669(2)	0.690 5(8)
O(1)	0.116 5(3)	0.011(1)	0.740 5(5)	0.117 3(4)	0.013(2)	0.744 1(7)
O(2)	−0.092 4(3)	0.509(2)	0.639 0(5)	0.092 2(4)	0.512(2)	0.634 0(7)
O(3)	−0.010 1(3)	0.417(2)	0.701 0(5)	−0.007 1(4)	0.413(2)	0.701 0(7)
O(4)	0.001 3(3)	0.393(1)	0.908 3(5)	−0.002 0(4)	0.386(2)	0.909 3(6)
O(5)	0.102 5(3)	0.577(1)	0.854 4(5)	0.102 5(5)	0.572(2)	0.851 7(7)
O(6)	0.233 7(3)	0.960(2)	0.711 0(5)	0.231 9(5)	0.960(2)	0.709 3(8)
O(7)	0.211 1(3)	0.451(1)	0.604 9(5)	0.211 0(4)	0.451(2)	0.606 2(6)
O(8)	0.123 1(3)	0.069(1)	0.535 8(5)	0.125 1(4)	0.067(2)	0.535 6(6)
O(9)	0.208 8(3)	0.413(1)	0.784 8(5)	0.210 7(5)	0.416(2)	0.789 2(7)
O(10)	0.294 6(3)	0.862(1)	0.586 0(4)	0.295 2(5)	0.575(2)	0.590 2(7)
O(11)	0.426 4(3)	−0.093(2)	0.577 5(5)	0.428 3(5)	−0.090(2)	0.577 7(6)
O(12)	0.382 6(3)	0.602(2)	0.410 5(5)	0.383 0(4)	0.600(2)	0.410 5(7)
O(13)	0.262 0(3)	0.952(1)	0.926 6(5)	0.261 4(5)	0.955(2)	0.925 1(7)
O(14)	0.316 0(3)	0.042(1)	0.428 7(5)	0.316 1(4)	0.039(2)	0.430 6(6)
O(15)	0.365 5(3)	0.407(1)	0.598 1(5)	0.366 2(4)	0.397(2)	0.600 0(7)
O(16)	0.596 0(3)	0.559(1)	0.741 4(4)	0.597 3(5)	0.560(2)	0.744 2(6)
O(17)	0.528 1(3)	0.011(2)	0.734 3(5)	0.526 7(4)	0.008(2)	0.733 4(6)
O(18)	0.491 2(3)	0.396(1)	0.582 3(5)	0.492 6(4)	0.391(2)	0.581 5(7)

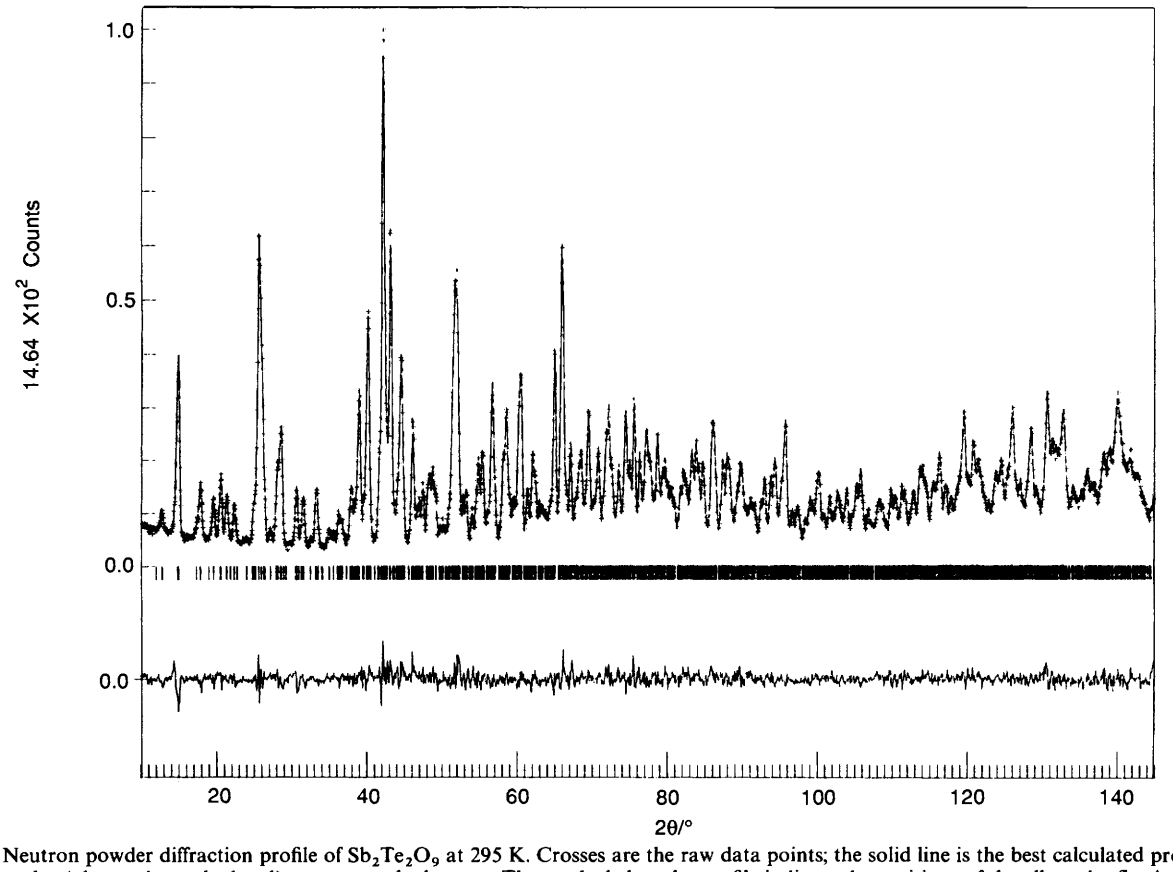

Fig. 1 Neutron powder diffraction profile of $Sb_2Te_2O_9$ at 295 K. Crosses are the raw data points; the solid line is the best calculated profile. The difference plot (observed − calculated) appears at the bottom. The marks below the profile indicate the positions of the allowed reflections (2667) included in the calculations

solved by X-ray single-crystal methods. The results are compared with those obtained from neutron powder diffraction data. The structural peculiarities are discussed within the general framework of the pentavalent antimony complex oxides, and compared with those of the known compounds in the M_2O_5–TeO_2 systems.

Table 3 Selected bond distances (Å) and angles (°) in $Sb_2Te_2O_9$

Sb(1)–O(1^{I})	1.912(7)	Sb(3)–O(15)	1.914(7)
Sb(1)–O(2)	1.934(8)	Sb(3)–O(11^{I})	1.924(6)
Sb(1)–O(3^{II})	1.982(8)	Sb(3)–O(12)	1.941(8)
Sb(1)–O(3)	1.989(7)	Sb(3)–O(10)	1.964(7)
Sb(1)–O(5)	2.016(6)	Sb(3)–O(14^{I})	1.973(7)
Sb(1)–O(4^{II})	2.030(6)	Sb(3)–O(13^{VIII})	2.024(6)
Sb(2)–O(1)	1.910(8)	Sb(4)–O(17^{V})	1.949(7)
Sb(2)–O(8)	1.941(7)	Sb(4)–O(11)	1.961(7)
Sb(2)–O(2)	1.952(7)	Sb(4)–O(17)	1.971(7)
Sb(2)–O(9)	1.956(6)	Sb(4)–O(15)	1.974(6)
Sb(2)–O(6^{III})	2.004(7)	Sb(4)–O(16^{VI})	1.998(7)
Sb(2)–O(7)	2.020(8)	Sb(4)–O(18)	2.015(8)
Te(1)–O(4)	1.869(7)	Te(3)–O(12)	1.877(8)
Te(1)–O(5)	1.890(8)	Te(3)–O(16^{VI})	1.890(6)
Te(1)–O(8)	1.895(6)	Te(3)–O(18^{VI})	1.903(7)
Te(1)–O(3^{II})	2.415(7)	Te(3)–O(18)	2.657(7)
Te(1)–O(4^{VII})	2.848(8)	Te(3)–O(17^{V})	2.740(8)
Te(1)–O(2^{IV})	3.079(7)	Te(3)–O(11^{V})	3.031(7)
Te(2)–O(14)	1.884(7)	Te(4)–O(6)	1.814(7)
Te(2)–O(13)	1.892(7)	Te(4)–O(10)	1.898(7)
Te(2)–O(9)	1.909(7)	Te(4)–O(7)	1.922(6)
Te(2)–O(10^{IV})	2.811(6)	Te(4)–O(9)	2.694(8)
Te(1)–O(2^{IV})	3.079(7)	Te(4)–O(15)	2.923(8)
O(1^{I})–Sb(1)–O(2)	93.8(3)	O(15)–Sb(3)–O(11^{I})	95.1(3)
O(1^{I})–Sb(1)–O(3^{II})	90.2(3)	O(15)–Sb(3)–O(12)	103.7(3)
O(1^{I})–Sb(1)–O(5)	89.3(3)	O(15)–Sb(3)–O(10)	86.9(3)
O(1^{I})–Sb(1)–O(4^{II})	89.8(3)	O(15)–Sb(3)–O(13^{VIII})	92.5(3)
O(2)–Sb(1)–O(3)	87.4(3)	O(11^{I})–Sb(3)–O(12)	90.2(3)
O(2)–Sb(1)–O(5)	103.0(3)	O(11^{I})–Sb(3)–O(10)	97.5(3)
O(2)–Sb(1)–O(4^{II})	83.6(3)	O(11^{I})–Sb(3)–O(14^{I})	89.2(3)
O(3^{II})–Sb(1)–O(3)	88.7(1)	O(12)–Sb(3)–O(14^{I})	84.9(3)
O(3^{II})–Sb(1)–O(5)	78.1(3)	O(12)–Sb(3)–O(13^{VIII})	86.9(3)
O(3^{II})–Sb(1)–O(4^{II})	93.4(3)	O(10)–Sb(3)–O(14^{I})	84.0(3)
O(3)–Sb(1)–O(5)	89.9(3)	O(10)–Sb(3)–O(13^{VIII})	84.0(3)
O(3)–Sb(1)–O(4^{II})	90.9(3)	O(14^{I})–Sb(3)–O(13^{VIII})	83.5(3)
O(1)–Sb(2)–O(8)	104.6(3)	O(17^{V})–Sb(4)–O(17)	92.0(2)
O(1)–Sb(2)–O(2)	92.5(3)	O(17^{V})–Sb(4)–O(15)	91.3(3)
O(1)–Sb(2)–O(9)	89.3(3)	O(17^{V})–Sb(4)–O(16^{VI})	83.4(3)
O(1)–Sb(2)–O(6^{III})	88.7(3)	O(17^{V})–Sb(4)–O (18)	93.8(3)
O(8)–Sb(2)–O(2)	92.6(3)	O(11)–Sb(4)–O(17)	84.9(3)
O(8)–Sb(2)–O(6^{III})	95.7(3)	O(11)–Sb(4)–O(15)	91.7(3)
O(8)–Sb(2)–O(7)	82.7(3)	O(11)–Sb(4)–O(16^{VI})	95.5(3)
O(2)–Sb(2)–O(9)	89.8(3)	O(11)–Sb(4)–O(18)	87.4(3)
O(2)–Sb(2)–O(7)	89.7(3)	O(17)–Sb(4)–O(16^{VI})	91.7(3)
O(9)–Sb(2)–O(6^{III})	81.3(3)	O(17)–Sb(4)–O(18)	89.5(3)
O(9)–Sb(2)–O(7)	83.3(3)	O(15)–Sb(4)–O(16^{VI})	88.8(3)
O(6^{III})–Sb(2)–O(7)	88.0(3)	O(15)–Sb(4)–O(18)	90.2(3)
O(4)–Te(1)–O(5)	95.1(3)	O(12)–Te(3)–O(16^{VI})	84.5(3)
O(4)–Te(1)–O(8)	93.6(3)	O(12)–Te(3)–O(18^{VI})	91.9(3)
O(5)–Te(1)–O(8)	88.0(3)	O(16^{VI})–Te(3)–O(18^{VI})	94.3(3)
O(14)–Te(2)–O(13^{III})	92.1(3)	O(6)–Te(4)–O(10)	90.0(3)
O(14)–Te(2)–O(9)	85.9(3)	O(6)–Te(4)–O(7)	100.1(3)
O(13^{III})–Te(2)–O(9)	95.1(3)	O(10)–Te(4)–O(7)	93.0(3)
Sb(1^{III})–O(1)–Sb(2)	138.0(4)	Sb(3^{III})–O(11)–Sb(4)	133.4(4)
Sb(1)–O(2)–Sb(2)	133.3(4)	Sb(3)–O(15)–Sb(4)	131.8(4)
Sb(1)–O(3)–Sb(1^{IX})	133.4(4)	Sb(4^{VI})–O(17)–Sb(4)	135.0(4)

Symmetry code: I $x, 1 + y, z$; II $-x, \frac{1}{2} + y, \frac{3}{2} - z$; III $x, y - 1, z$; IV $x, \frac{3}{2} - y, \frac{1}{2} + z$; V $1 - x, \frac{1}{2} + y, \frac{3}{2} - z$; VI $1 - x, y - \frac{1}{2}, \frac{1}{2} - z$; VII $-x, 1 - y, 2 - z$; VIII $x, \frac{3}{2} - y, z - \frac{1}{2}$; IX $-x, y - \frac{1}{2}, \frac{3}{2} - z$

Table 4 Bond valences for Sb–O and Te–O in $Sb_2Te_2O_9$ *

Atom	1	2	3	4	5	6	ΣS
Sb(1)	1.91	1.93	1.98	1.99	2.02	2.03	
	1.00	0.93	0.80	0.79	0.73	0.70	4.95
Sb(2)	1.91	1.94	1.95	1.96	2.00	2.02	
	1.00	0.91	0.88	0.87	0.75	0.72	5.13
Sb(3)	1.91	1.92	1.94	1.96	1.97	2.02	
	0.99	0.96	0.91	0.85	0.83	0.71	5.25
Sb(4)	1.95	1.96	1.97	1.97	2.00	2.02	
	0.89	0.86	0.83	0.82	0.77	0.73	4.90
Te(1)	1.87	1.89	1.90	2.42	2.85	3.08	
	1.28	1.21	1.19	0.34	0.14	0.10	4.26
Te(2)	1.88	1.89	1.91	2.81	2.96		
	1.23	1.20	1.15	0.15	0.12		3.85
Te(3)	1.88	1.89	1.90	2.66	2.74	3.03	
	1.25	1.21	1.16	0.21	0.18	0.10	4.11
Te(4)	1.81	1.90	1.92	2.69	2.92		
	1.49	1.18	1.11	0.19	0.13		4.10

* Values are d(M–O) followed by S_M where $S_{Sb} = (d/1.911)^{-6.0}$ from ref. 14 and [b] $S_{Te} = 1.333\,(d/1.854)^{-5.2}$ from ref. 15.

Experimental

Preparation.—Polycrystalline $Sb_2Te_2O_9$ was prepared as described elsewhere.[7] Single crystals were obtained by means of a transport reaction, using $TeCl_4$ as the transport agent. A mixture of powdered $Sb_2Te_2O_9$ (1 g) and $TeCl_4$ (50 mg) was heated in a sealed evacuated Vycor ampoule (diameter 12 mm, length 30 cm) in a temperature gradient of 750–650 °C for 3 d. Colourless needles (length 2 mm, average width 0.2 mm) were found in the cold extremity of the ampoule. They were successively washed in HCl and distilled water, and then dried at 80 °C.

X-Ray Diffraction.—The data collection was performed using an Enraf-Nonius CAD4 diffractometer. Table 1 shows physical and crystallographic data together with the experimental conditions of data collection.

The structure was determined by the Patterson method. The distinction between Sb and Te atoms was facilitated by the oxygen environment, with six homogeneous bonds around Sb. The refinements were carried out by full-matrix least-squares calculations. Atomic scattering factors were corrected for anomalous dispersion.[9] Calculations were performed with SHELX[10] using an ALLIANT VF-80 computer.

Additional material available from the Cambridge Crystallographic Data Centre comprises thermal parameters and remaining bond lengths and angles.

Neutron Diffraction.—Neutron powder diffraction data were collected in the high-resolution D2B diffractometer at the Institut Laue-Langevin (ILL)-Grenoble, using a wavelength of 1.594(1) Å. About 10 g of sample were enclosed in a vanadium can of 8 mm diameter. The pattern was collected at 295 K in the angular range $0 \leqslant 2\theta \leqslant 150°$, in steps of 0.05°.

The neutron diffraction profile was analysed by the Rietveld[11] method, using the DBW[12] refinement program. The line shape of the diffraction peaks was generated with a pseudo-Voigt function. The coherent scattering lengths for Sb, Te and O were 5.641, 5.430 and 5.805 fm, respectively.

The regions $0 \leqslant 2\theta \leqslant 10$ and $145 \leqslant 2\theta \leqslant 150°$ were excluded in the refinement. A total of 121 parameters were refined, including six background coefficients, zeropoint, half-width, pseudo-Voigt and asymmetry parameters for the peak shape, scale factor, positional, thermal isotropic and unit-cell parameters. The maximum shift-to-error value for an atomic coordinate in the final refinement cycle was $\delta/\sigma = 0.05$.

Results

X-Ray Diffraction.—The final positional parameters are given in Table 2, and Table 3 lists selected bond distances and angles.

Neutron Powder Diffraction.—The refinement of the neutron

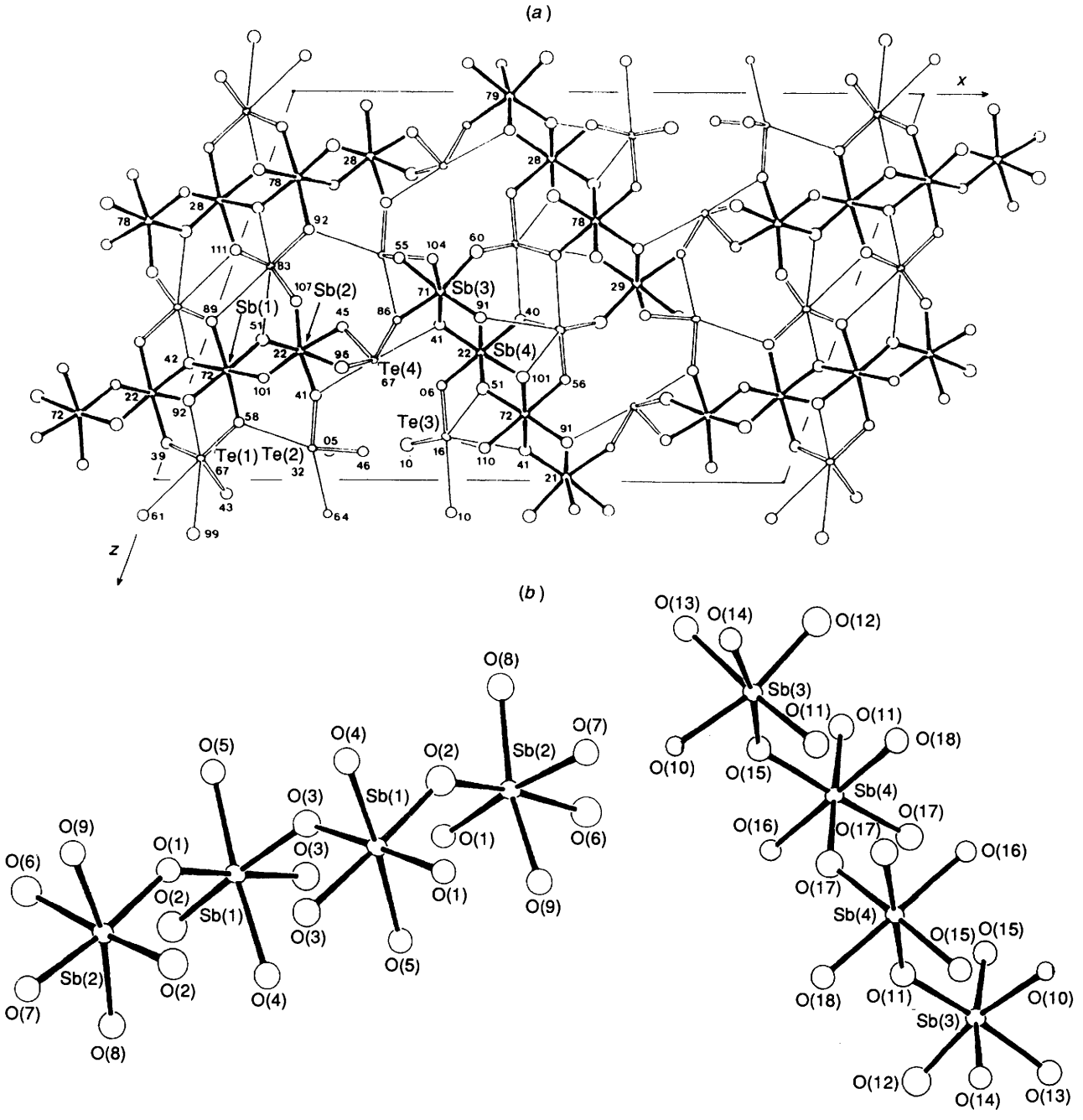

Fig. 2 (*a*) [0 1 0] Projection of the $Sb_2Te_2O_9$ structure. Thick lines represent Sb–O bonds, very thin lines Te–O bonds at distances betewen 2.0 and 3.1 Å. (*b*) Antimony environments

pattern according to the structural model determined from X-ray data led to the final atomic parameters also included in Table 2. Fig. 1 shows the agreement between the observed and calculated profiles. Final discrepancy factors R_p, R_{wp}, R_{exptl}, and χ^2 (defined in ref. 11) were 4.88, 6.39, 4.73, and 1.82, respectively. The R_I factor for the integrated intensities was 3.77 for 2667 reflections. The neutron results do not show any significant structural deviations from the X-ray model; the differences in atomic parameters are, in general, lower than two times the standard deviation for the metallic atoms, and four times for the oxygens. A X–N Fourier difference map[13] did not permit localization of well defined residual electronic density in the proximities of the Te atoms (lone pairs), probably due to the large scattering factor of both Sb and Te atoms present in the structure.

The structural description that follows refers to the data obtained from the X-ray single-crystal study.

Description of the Structure.—In the unit cell there are four crystallographically inequivalent antimony and tellurium atoms. Fig. 2 shows a view of the structure projected along the [0 1 0] axis. All the Sb atoms are co-ordinated to six oxygens forming quasi-regular octahedra. The Sb–O distances range from 1.91 to 2.03 Å with an average of 1.98 Å for Sb(1) and Sb(4) and 1.96 Å for Sb(2) and Sb(3). The SbO_6 octahedra share corners to give infinite quadruple chains parallel to the *b* axis (Fig. 3). As it can be seen in Fig. 3(*a*), there exist two crystallographically non-equivalent chains. The first is built up by Sb(1) and Sb(2) octahedra (chain A), connected *via* O(1), O(2) and O(3); the second contains the Sb(3) and Sb(4) octa-

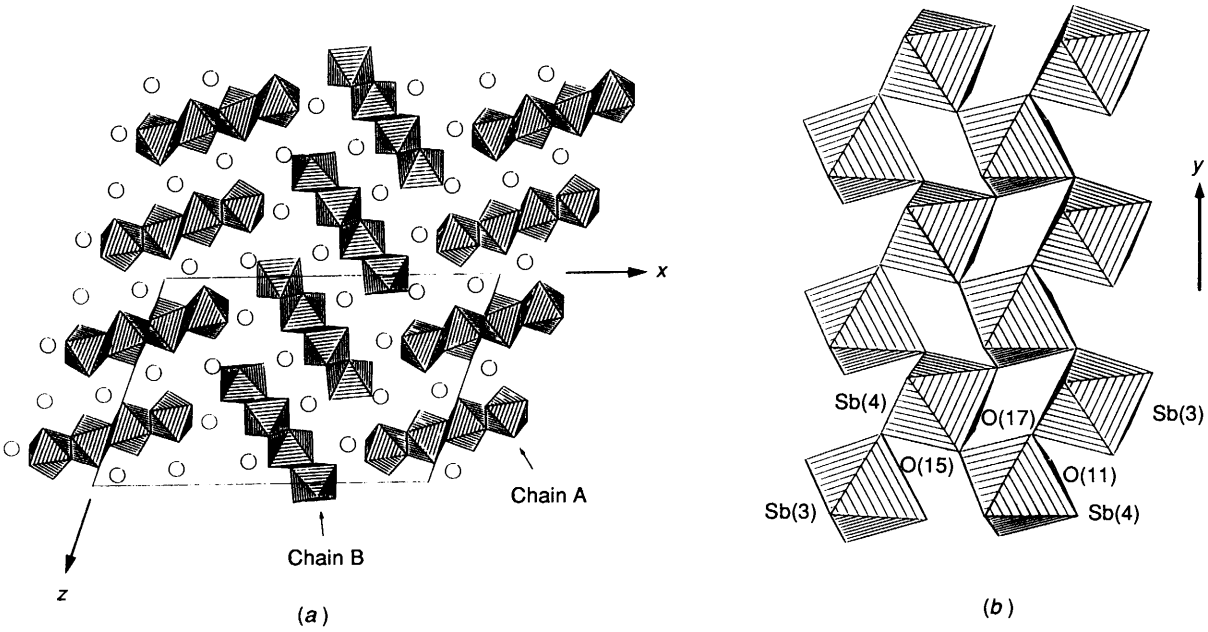

Fig. 3 Two views of the quadruple chains of vertex-sharing SbO_6 octahedra: (*a*) [0 1 0] projection, (*b*) view perpendicular to a single chain (chain B)

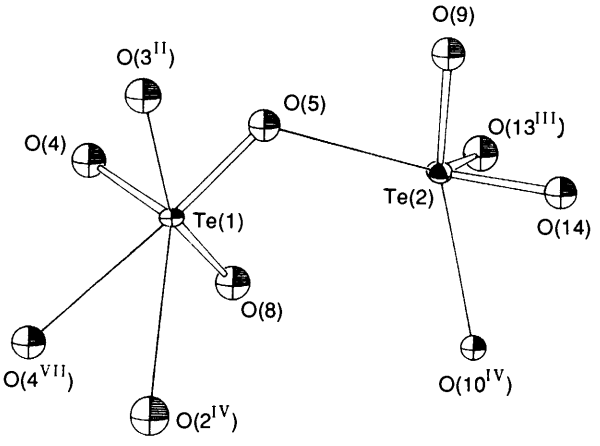

Fig. 4 Oxygen co-ordination polyhedra of five- and six-co-ordinated Te(1) and Te(2). Thin lines correspond to Te–O bonds at distances between 2.0 and 3.1 Å

hedra (chain B), bonded through O(11), O(15) and O(17). The angle between the chains is 107°. Brown's bond valences[14] for Sb–O bonds, listed in Table 4, sum to a value close, on average, to the expected valence for antimony in this compound.

The co-ordination number of the Te atoms can be discussed in terms of bond valence theory.[14] Table 4 includes the valences associated with the oxygens bonded to Te at distances lower than 3.1 Å. Following Brown's criterion, largely applied by Philipot in many tellurium compounds,[15] for distances larger than 3.1 Å the Te–O interactions can be neglected, the bond valences taking values lower than 0.09. In $Sb_2Te_2O_9$ each Te atom is strongly bonded to three oxygens, at distances between 1.81 and 1.92 Å, in a trigonal-pyramidal configuration. According to Table 4, Te(1) and Te(3) are also co-ordinated to three other oxygen atoms, in a very irregular environment allowing room for the electronic lone pair. In the same way Te(2) and Te(4) are bonded to two additional oxygens in a ψ-octahedral configuration, where the inert pair is thought to occupy the sixth vertex. Fig. 4 shows the tellurium environment for both kinds of oxygen co-ordination.

In this way, Te atoms are grouped together by means of the weakest bonds corresponding to distances between 2.42 and 3.08 Å. Atoms Te(2) and Te(4) are linked *via* O(9) and O(10) to give infinite strings parallel to the [0 0 1] direction. Bridges O(5)–Te(1)–O(4)–Te(1)–O(5) link neighbouring chains, giving rise to infinite double strings, of composition $(Te_6O_{26})_\infty$. On the other hand, pairs of Te(3) atoms are bonded *via* O(18), forming isolated two-fold groups Te_2O_{10} (Fig. 5). Both kinds of tellurium groups hold together the four-fold strings of SbO_6 octahedra.

Discussion

Tellurium Network.—The association of tellurium co-ordination units in $Sb_2Te_2O_9$, giving rise to double strings of composition $(Te_6O_{26})_\infty$, is intermediate between those found in the isostoichiometric compounds of V and Ta,[2,4] as expected.

Considering the tellurium(IV) lone pair as a sphere with a volume similar to that of an oxygen atom,[1] the average volume per anion in $Sb_2Te_2O_9E_2$ (E = lone pair) is 16.5 Å^3. As a comparison, the values for $V_2Te_2O_9$, Nb_2TeO_9 and $Ta_2Te_2O_9$ are 15.6, 17.2 and 17.2 Å^3, respectively. This implies the existence of vacant sites in the structure, which are physically occupied by the electron pair. These sites are in the neighbourhood of each Te atom, as it can be seen in Fig. 2.

Antimony Network.—Pentavalent antimony forms a large variety of $ASbO_x$ complex oxides[16] with very different elements A. All of these compounds are based on octahedral SbO_6 co-ordination groups, which are linked together, *via* common vertices or edges, to give $(Sb_nO_m)_\infty$ two- or three-dimensional nets. The aggregation degree of the SbO_6 octahedra, proportional to the number of common oxygens, depends on the chemical nature of the elements A: with electropositive metals the aggregation degree of such polyhedra tends to be higher.

It is useful to define a coefficient giving a quantitative idea of the degree of association of MO_p polyhedra in a net characterized by a repeating unit of formula M_nO_m. The aggregation factor (a.f.) can be defined as $2[p - (m/n)]/p$. For instance, *a.f.* = 0 for isolated polyhedra, without common oxygens, and 1 for a three-dimensional network in which each MO_p polyhedron shares p corners with p similar polyhedra (repeating unit $MO_p/2$).

In the crystallochemistry of pentavalent antimony there are a large number of examples of complex oxides defined by a repeating unit $(Sb_qO_{3q})_\infty$ (q = 1, 2, etc.), a.f. = 1, such as $KSbO_3$ (ilmenite structure), $AlSbO_4$ (random rutile), $Ag_2Sb_2O_6$ (pyrochlore) or $Cd_2Sb_2O_7$ (weberite).[16] Only for more

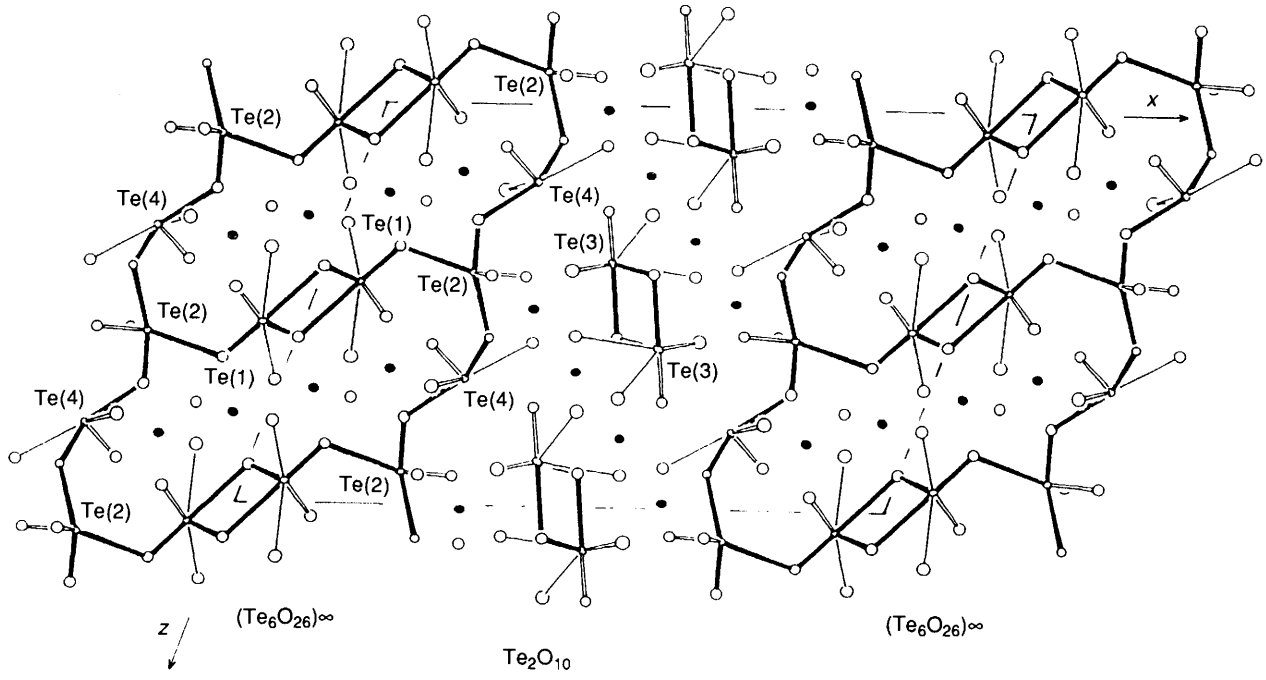

Fig. 5 [0 1 0] Projection showing the strings $(Te_6O_{26})_\infty$ and the groups Te_2O_{10}. Black dots are Sb atoms. For the sake of clarity, Sb–O bonds are not drawn

electronegative elements, such as Sb itself, in Sb_2O_4 (*i.e.* $Sb^{III}Sb^{V}O_4$) can the layered structure of both α and β polymorphs[17] be described by a repeating unit $(Sb_2O_8)_\infty$, implying a lower aggregation factor, a.f. = 0.66.

In $Sb_2Te_2O_9$, the tellurium electronegativity being still lower (Allred–Rochow[18] electronegativities for Sb and Te are 1.82 and 2.01, respectively), the SbO_6 antimony octahedra are still less associated. The repeating unit for the four-fold strings is $(Sb_4O_{17})_\infty$, with a.f. = 0.58. There are no examples, to our knowledge, of pentavalent antimony complex oxides containing p elements more electronegative than tellurium. The lowest limit of association of SbO_6 octahedra seems to be that found in the $Sb_2Te_2O_9$ structure.

It is also interesting to compare the M–O nets of the known M_2O_5–TeO_2 oxides. In $V_2Te_2O_9$[2] five-co-ordinated vanadium atoms occupy the centre of trigonal bipyramids, which share corners to give infinite one-dimensional $(VO_4)_\infty$ strings, with a.f. = 0.40. The NbO_6 octahedra share vertices in $Nb_2Te_3O_{11}$,[3] to give double infinite one-dimensional chains $(Nb_2O_9)_\infty$, a.f. = 0.50. As for $Ta_2Te_2O_9$,[4] TaO_6 octahedra are linked *via* common vertices forming a two-dimensional network $(Ta_4O_{16})_\infty$, a.f. = 0.66. The aggregation degree found in $Sb_2Te_2O_9$ is intermediate between those of the compounds of V and Ta. The comparison with $Nb_2Te_3O_{11}$ is not strictly correct since the M/Te ratio is lower in this compound: the hypothetical oxide $Nb_2Te_2O_9$ probably would show a higher degree of association of the NbO_6 octahedra. The different stacking of polyhedra along the sequence chains, quadruple chains, layers can be explained as a consequence of the gradual increase in the ionic character of the M–O bonds for M = V, Sb, Ta.

There are many examples of isostoichiometric complex oxides of Nb^V and Ta^V which crystallize in structures quite different from that of the corresponding antimony(v) compound [*e.g.* $LiSbO_3$ (space group *Pncn*) *vs.* $Li(Nb,Ta)O_3$ (*R*3*c*)]. This fact cannot be attributed to differences in electrostatic Madelung energy, since the three cations have similar formal valences and sizes. Goodenough and Kafalas[19] propose that the covalent contribution to the M–O bonds (M = Sb, Nb or Ta) is responsible for the observed differences. Covalent σ bonding of an oxygen to two near-neighbour cations is stronger if these cations are on the same side of the oxygen, which allows the participation of two oxygen p orbitals, and favours M–O–M angles close to 90°. This is the predominant covalent contribution to the M–O bond for Sb^V, which has a filled d^{10} core that cannot participate in π bonding to p orbitals of the neighbouring oxygens. On the contrary, Nb^V and Ta^V have empty d shells that participate in covalent bonding to oxygens. The anion p orbitals are shared between both covalent contributions, which weakens the σ bonding and favours 180° O–M–O angles. In consequence, Nb and Ta stabilize different crystal structures from those of Sb.

In the $Sb_2Te_2O_9$ structure the SbO_6 octahedra that constitute the quadruple chains are strongly tilted, showing Sb–O–Sb angles in the range 131.8–138.0° [see Table 2 and Fig. 3(b)], far away from 180°. This is thought to be due to the strong σ covalent contribution to the Sb–O bonding which tends to adjust the angles towards 90°. Lower angles would involve strong repulsions between pentavalent antimony cations. On the contrary, the NbO_6 octahedra in $Nb_2Te_3O_{11}$ are scarcely rotated, with Nb–O–Nb angles of 171.0 or 168.0°. This is also true for $Ta_2Te_2O_9$, which exhibits Ta–O–Ta angles of 145.5 or 180.0°. Both cases show clearly the partial inhibition of the σ bonding. Thus, the covalent binding energy seems to play a major role in stabilizing the $Sb_2Te_2O_9$ structure.

Acknowledgements

The authors thank Dr. J. L. Soubeyroux for the collection of the neutron diffraction diagram, and the ILL for making all facilities available. A. C. thanks the Ministerio de Educación y Ciencia of Spain and the Centre National de la Recherche Scientifique of France for support.

References

1 J. Galy, G. Meunier, S. Andersson and A. Astrom, *J. Solid State Chem.*, 1975, **13**, 142.
2 J. Darriet and J. Galy, *Cryst. Struct. Commun.*, 1973, **2**, 237.
3 J. Galy and O. Lindqvist, *J. Solid State Chem.*, 1979, **27**, 279.
4 J. A. Alonso, A. Castro, E. Gutiérrez Puebla, M. A. Monge, I. Rasines and C. Ruiz Valero, *J. Solid State Chem.*, 1987, **69**, 36.
5 C. Pico, A. Castro, M. L. Veiga, E. Gutiérrez Puebla, M. A. Monge and C. Ruiz Valero, *J. Solid State Chem.*, 1986, **63**, 172.
6 A. Castro, R. Enjalbert, D. Lloyd, I. Rasines and J. Galy, *J. Solid State Chem.*, 1990, **85**, 100.

7 J. A. Alonso, A. Castro, A. Jerez, C. Pico and M. L. Veiga, *J. Chem. Soc., Dalton Trans.*, 1985, 2225.
8 N. Walker and D. Stuart, *Acta Crystallogr., Sect. A*, 1983, **39**, 158.
9 D. T. Cromer and J. Waber, *International Tables for X-Ray Crystallography*, Kynoch Press, Birmingham, 1974, vol. 4.
10 G. M. Sheldrick, SHELX 76, Program for Crystal Structure Determination, University of Cambridge, 1976.
11 H. M. Rietveld, *J. Appl. Crystallogr.*, 1969, **2**, 65.
12 R. A. Young and D. B. Wiles, *J. Appl. Crystallogr.*, 1982, **15**, 430.
13 P. Coppens, *Top. Curr. Phys.*, 1978.
14 I. D. Brown, *Structure and Bonding in Crystals*, eds. M. O'Keefe and A. Navrotsky, Wiley, New York, 1981, vol. 2.
15 E. Philippot, *J. Solid State Chem.*, 1981, **38**, 26.
16 A. F. Wells, *Structural Inorganic Chemistry*, Clarendon Press, Oxford, 1984.
17 J. Amador, E. Gutiérrez Puebla, M. A. Monge, I. Rasines and C. Ruiz Valero, *Inorg. Chem.*, 1988, **27**, 1367.
18 A. L. Allred and E. G. Rochow, *J. Inorg. Nucl. Chem.*, 1958, **5**, 264.
19 J. B. Goodenough and J. A. Kafalas, *J. Solid State Chem.*, 1973, **6**, 493.

Received 18*th March* 1992; *Paper* 2/01436J